(*2R,6R*)-hydroxynorketamine rapidly potentiates optically-evoked Schaffer collateral synaptic activity

Lace M. Riggs[a,b,g], **Scott M. Thompson**[b,c], **Todd D. Gould**[b,d,e,f]

[a]Program in Neuroscience and Training Program in Integrative Membrane Biology, University of Maryland School of Medicine, Baltimore, MD 21201, USA;

[b]Department of Psychiatry, University of Maryland School of Medicine, Baltimore, MD 21201, USA;

[c]Department of Physiology, University of Maryland School of Medicine, Baltimore, MD 21201, USA;

[d]Department of Pharmacology, University of Maryland School of Medicine, Baltimore, MD 21201, USA;

[e]Department of Anatomy and Neurobiology, University of Maryland School of Medicine, Baltimore, MD 21201, USA;

[f]Veterans Affairs Maryland Health Care System, Baltimore, MD 21201, USA;

Abstract

(*2R,6R*)-hydroxynorketamine (HNK) is a metabolite of ketamine that exerts rapid and sustained antidepressant-like effects in preclinical studies. We hypothesize that the rapid antidepressant actions of (*2R,6R*)-HNK involve an acute increase in glutamate release at Schaffer collateral synapses. Here, we used an optogenetic approach to assess whether (*2R,6R*)-HNK promotes glutamate release at CA1-projecting Schaffer collateral terminals in response to select optical excitation of CA3 afferents. To do this, the red-shifted channelrhodopsin, ChrimsonR, was expressed in dorsal CA3 neurons of adult male Sprague Dawley rats. Transverse slices were collected four weeks later to determine ChrimsonR expression and to assess the acute synaptic effects of an antidepressant-relevant concentration of (*2R,6R*)-HNK (10 μM). (*2R,6R*)-HNK led to a rapid potentiation of CA1 field excitatory postsynaptic potentials evoked by recurrent optical stimulation of ChrimsonR-expressing CA3 afferents. This potentiation is mediated in part by an increase in glutamate release probability, as (*2R,6R*)-HNK suppressed paired-pulse facilitation at CA3 projections, an effect that correlated with the magnitude of the (*2R,6R*)-HNK-induced potentiation of CA1 activity. These results demonstrate that (*2R,6R*)-HNK increases the probability of glutamate release at CA1-projecting Schaffer collateral afferents, which may be involved in the antidepressant-relevant behavioral adaptations conferred by (*2R,6R*)-HNK *in vivo*. The current study also establishes proof-of-principle that genetically-encoded light-sensitive

proteins can be used to investigate the synaptic plasticity induced by novel antidepressant compounds in neuronal subcircuits.

Keywords

Hippocampus; Optogenetics; Ketamine; Hydroxynorketamine; Glutamate; Depression; Plasticity

1. INTRODUCTION

Depression is an often-debilitating condition that traditional antidepressants cannot always address (Riggs and Gould, 2021). Clinical studies have shown that a single subanesthetic dose of ketamine can rapidly alleviate symptoms of major depression (Berman et al., 2000), even in patients who do not respond to other forms of treatment (Zarate et al., 2006). This led the United States Food and Drug Administration to approve the (*S*)-ketamine stereoisomer for patients who suffer from either acute suicidality or who repeatedly fail to respond to traditional antidepressant approaches (Cristea and Naudet, 2019). The ketamine discovery helped invigorate the pursuit of next-generation antidepressants (Skolnick et al., 2009) and altered the trajectory of neuropsychiatric research (Zarate, 2021), especially with regard to understanding rapid antidepressant mechanisms of action (Abdallah et al., 2018; Duman et al., 2019; Hashimoto, 2019; Hess et al., 2021; Murrough et al., 2017; Riggs and Gould, 2021). However, ketamine is a dissociative anesthetic that has dose-dependent side-effects (Krystal et al., 1994), mediated in part, via *N*-methyl-D-aspartate receptor (NMDAR) blockade (Zanos et al., 2018) – a mechanism that does not on its own yield 'ketamine-like' antidepressant effects (Gould et al., 2019; Lener et al., 2017; Newport et al., 2015). While clear guidelines are now provided for the ethical use of ketamine for the treatment of depression (McIntyre et al., 2021), there is still a need to identify novel rapid-acting antidepressant compounds that have improved safety and tolerability.

Several glutamatergic modulators are now under preclinical and clinical development for depression (Chaki, 2020; Henter et al., 2021; Riggs and Gould, 2021; Witkin et al., 2019), including ketamine's own bioactive metabolites (ClinicalTrials.gov Identifier: NCT04711005) (Highland et al., 2021, 2022). Preclinical studies have shown that the (*2R,6R*)-hydroxynorketamine (HNK) ketamine metabolite exerts rapid and sustained antidepressant-like actions (Zanos et al., 2016), but with minimal adverse effects relative to ketamine itself (Highland et al., 2018; Zanos et al., 2016). In the hippocampus, (*2R,6R*)-HNK rapidly potentiates α-amino-3-hydroxy-5-methyl-4-isoxazolepropionic acid receptor (AMPAR)-mediated activity (Riggs et al., 2020; Zanos et al., 2016), in part, by promoting glutamate release at Schaffer collateral synapses independent of acute changes in AMPAR function, NMDAR blockade, or network disinhibition (Riggs et al., 2020). However, prior studies have only used electrical field stimulation, and so activation of other synaptic inputs may functionally contribute to this Schaffer collateral plasticity despite otherwise appearing to be synapse-specific (Riggs et al., 2020). This is because Schaffer collateral activity is also modulated by axonal varicosities from the dorsal raphe and locus coeruleus (Andersen et al., 2006) and (*2R,6R*)-HNK administration has been shown to potentiate both serotonin and norepinephrine release (Ago et al., 2019; Pham et al., 2018). Thus, while we predict that

the electrically-evoked plasticity induced by (*2R,6R*)-HNK at Schaffer collateral synapses is due to a potentiation of glutamate release from CA1-projecting CA3 terminals, it is possible that (*2R,6R*)-HNK may be exerting these effects indirectly by potentiating the activity of monoaminergic inputs onto Schaffer collateral synapses. In the current study, we used a combined optogenetic and electrophysiological approach to assess whether (*2R,6R*)-HNK promotes glutamate release at CA1-projecting Schaffer collateral terminals in response to select optical excitation of CA3 afferents – an effect that could have important implications with regard to its broader actions throughout the mesocorticolimbic circuit. Our study establishes proof-of-principle that cell-type specific expression of genetically-encoded light-sensitive proteins can be used to investigate the rapid synaptic effects of antidepressants with subcircuit-level specificity.

2. MATERIALS AND METHODS

2.1. Animals

Four-week-old male Sprague Dawley rats (Charles River Laboratories, MA) were acclimated to the vivarium (University of Maryland, Baltimore, MD) for one week prior to experiments. Rats were housed three per cage under standard conditions (12-h light-dark cycle; lights on at 7:00AM) and with food and water available *ad libitum*. All experimental procedures were approved by the University of Maryland Baltimore Animal Care and Use Committee and were conducted in full accordance with the National Institutes of Health Guide for the Care and Use of Laboratory Animals.

2.2. Compounds

(*2R,6R*)-hydroxynorketamine (HNK) HCl was synthesized by the National Center for Advancing Translational Sciences (Bethesda, MD) and absolute and relative stereochemistry was confirmed by small molecule x-ray crystallography as previously described (Morris et al., 2017). (*2R,6R*)-HNK was prepared as a 10 mM stock solution in purified milli-q water on the day of the experiment and then diluted to a final concentration of 10 μM in artificial cerebrospinal fluid (ACSF) during the experiment. This concentration is consistent with peak hippocampal concentrations following systemic administration of (*2R,6R*)-HNK at an antidepressant-relevant dose (Lumsden et al., 2019) which also potentiates electrically-evoked Schaffer collateral activity (EC50 = 3.3 μM; Riggs et al., 2020).

2.3. Surgery

Rats were anesthetized with isoflurane using a precision vaporizer (3.5% in O_2). Once anesthetized, rats were placed onto a stereotaxic frame (David Kopf Instruments, Tujunga, CA) and anesthesia was maintained (2% in O_2) through a nose-cone for the remainder of the surgery. A 33-gauge syringe (Hamilton Company, Reno, NV) was used to inject 0.3 μL of pAAV-Syn-ChrimsonR-tdT (Klapoetke et al., 2014) into the CA3 region of the dorsal hippocampus (−3.3 mm anterior/posterior; 3.7 mm medial/lateral; −3.7 dorsal/ventral). Rats were then returned to the vivarium for four weeks to allow for full recovery and viral expression prior to electrophysiology experiments (Figure 1). pAAV-Syn-ChrimsonR-tdT was obtained from Addgene and deposited by Dr. Edward Boyden (Addgene plasmid #59171-AAV9; http://n2t.net/addgene:59171; RRID:Addgene_59171).

2.4. Histology

Expression of ChrimsonR-tdT was validated with fluorescent microscopy in a subset of rats that were not used for electrophysiology experiments. Briefly, rats were anesthetized with vaporized isoflurane (3.5% in O_2) and then perfused with 4% paraformaldehyde in phosphate buffered saline. Brains were then extracted and post-fixed for one day at 4°C in 4% paraformaldehyde. A vibratome was used to collect 50-μm coronal sections which were then washed for 15 min in 1% phosphate buffered saline before mounting onto slides with DAPI-containing VectaShield Antifade Mounting Medium (Vector Laboratories Inc, Burlingame, CA). Images were acquired on a Leica DM6 microscope with DAPI (460 nm) and Cyanine3 (610 nm) filters using the LASX imaging software.

2.5. Electrophysiology

Dissecting and recording ACSF contained (in mM): 120 NaCl, 3 KCl, 1 NaH$_2$PO$_4$, 25 NaHCO$_3$, 1.5 MgSO$_4$·7H$_2$O, 2.5 CaCl$_2$, and 20 D-glucose, and was carbogenated with 95% O_2 and 5% CO_2. Standard methods were used to prepare transverse hippocampal slices (400-μm thickness). To select for dorsal hippocampal slices containing ChrimsonR-tdT expression, sections were collected under dim-lighting conditions along the dorsal-ventral hippocampal axis (Figure 1). Upon sectioning, each slice was arranged sequentially onto an ACSF interface in a humidified holding chamber that was covered to prevent light penetration. Once slices had recovered for at least an hour, the dorsal-most slice was then transferred to a submersion-type recording chamber and superfused at a rate of 1.5 mL/min at room temperature (20–22°C). ChrimsonR-tdT expression was confirmed using a HQ610 Chroma filter on a Nikon Eclipse E400 and excitatory postsynaptic potentials were evoked using a fiber-coupled 625 nm LED (Thorlabs Inc, Newton, NJ). To proceed in an experiment, a given slice had to exhibit: (*a*) a pattern of ChrimsonR-tdT expression that was spatially restricted to CA3 and (*b*) a measurable excitatory postsynaptic potential in CA1 in response to the minimum light intensity (0.1 A). An input-output relationship was generated in 0.2-A current steps and 150% of threshold was used to stimulate CA3 afferents over time (1 ms duration, 0.05 Hz interval, 5 mW/mm^2 irradiance) to assess the synaptic effects of bath-applied (*2R,6R*)-HNK (10 μM). ACSF-filled recording pipettes (3–5 MΩ) were placed in the *stratum radiatum* of CA1 to record optically-evoked field excitatory postsynaptic potentials (fEPSPs).

The pClamp 11 Software Suite (Molecular Devices, LLC, San Jose, CA) was used to analyze fEPSP slope (mV/ms), defined as the rising phase of the response (1.25 ms) immediately following the presynaptic fiber volley. Responses are plotted as a function of time and reflect the mean of three consecutive sweeps. Comparisons were made using the averaged response at the end of the recording period for each group ($t = 25$–30 min, respectively). The change in fEPSP was calculated and plotted as a change from baseline (Equation 1). Paired pulse stimuli were generated using a 50-ms interstimulus interval at the end of the baseline recording period and during the last minute of test compound superfusion. Paired pulse ratios were calculated from the mean of five consecutive sweeps and the change in paired pulse was calculated as a change from baseline (Equation 2):

$$fEPSP \left(\frac{mV}{ms}[\%]\right) = \frac{mV/ms_{(test\ pulse)}}{mV/ms_{(baseline\ \bar{x})}} \times 100 \qquad (1)$$

$$\Delta PPR = \frac{P2_{(PPR\ after\ test\ compound)} - P1_{(PPR\ at\ baseline)}}{P1_{(PPR\ at\ baseline)}} \times 100 \qquad (2)$$

All experiments were completed within four hours of slice collection. Data from each slice were included in the final analyses if they exhibited: (*a*) a stable fEPSP during baseline, defined as <10% variation in either direction from its initial slope, (*b*) a stable fEPSP during baseline, defined as <15% variation from central tendency, and (*c*) a stable presynaptic fiber volley across the duration of the recording, defined as <15% variation in either direction from its initial amplitude. Inclusion criteria were determined *a priori* based on prior studies (Riggs et al., 2020) and the slice-by-slice determination as to whether these criteria were met were established *a posteriori* during the data analysis and prior to unblinding.

2.6. Statistical Analyses

All experiments were performed in a randomized fashion and conducted and analyzed by an experimenter who was blind to the drug conditions. A single slice is considered a single replicate (*n*) and drug condition was randomly assigned in a blinded fashion on a slice-by-slice basis for each rat. Data were analyzed with GraphPad Prism Software 9.3.0 and assessed for normality (Shapiro-Wilk) and homogeneity of variance (*F*-test). Data are presented as mean ± standard error of the mean and statistical significance was defined as $p < 0.05$. Two-way repeated measures analysis of variance was used to assess an effect of drug bath application as a function of time. When parametric assumptions were met, unpaired two-tailed *t*-tests were used for between-group comparisons. The Mann-Whitney U test was used as a non-parametric alternative when parametric assumptions were not met. Using standard criteria (Cohen, 1992, 1988), effect sizes were defined as small (0.2), medium (0.5), or large (0.8), and determined by: (*a*) Cohen's *d* when comparisons were of equal sample size and standard deviation, (*b*) Glass' *delta* when comparisons were of equal sample size but differed in standard deviation, or (*c*) Hedges' *g* when comparisons were of unequal sample size regardless of standard deviation. Grubbs' ($p < 0.05$) was used to detect statistically significant outliers.

3. RESULTS

We used an optogenetic approach to assess whether (*2R,6R*)-HNK potentiates glutamate release at Schaffer collateral synapses. The red-shifted channelrhodopsin, ChrimsonR, was injected into the CA3 subregion of the adult male Sprague Dawley rat dorsal hippocampus via a slow (0.025 μl/min) low-volume (0.3 μl) infusion. ChrimsonR-tdT expression was assessed four weeks later (Figure 1). We observed spatially restricted ChrimsonR-tdT expression in the CA3 subfield of the dorsal hippocampus (Figure 2).

ChrimsonR-expressing CA3 afferents in *stratum radiatum* were optically stimulated in *ex vivo* dorsal hippocampal transverse slices and excitatory postsynaptic potentials were recorded in CA1 *stratum radiatum* (Figure 1). CA1 excitatory postsynaptic potentials

increased predictably with increasing intensity of light stimulation (Figure 3A). The range of light stimulation intensities used here appeared to maximally excite ChrimsonR-expressing fibers toward the higher end of the stimulation range (Figure 3B), indicating a saturation of ChrimsonR-evoked currents in presynaptic fibers (Glasgow et al., 2019), and thus 150% of threshold was used to stimulate CA3 afferents over time (1 ms duration, 0.05 Hz interval, 5 mW/mm2 irradiance) to assess the synaptic effects of (*2R,6R*)-HNK. When assessing the effect of bath-applied vehicle (VEH) vs. (*2R,6R*)-HNK on the change in CA1 excitatory postsynaptic potentials over time, we observed a significant main effect of drug ($F_{(1,12)}$ = 11.54, p = 0.0053) and time ($F_{(34,396)}$ = 3.860, $p < 0.0001$), as well as a significant drug × time interaction ($F_{(34,396)}$ = 2.637, $p < 0.0001$) (Figure 4A, *left panel*). When assessing mean differences during the last five minutes of bath application (t = 25–30 min; Figure 4A, *right panel*), we observed a significant difference in the between-group variance ($F_{(6,6)}$ = 8.640, p = 0.0190), in which (*2R,6R*)-HNK led to a significant and large-effect potentiation of optically-evoked responses relative to VEH-exposed slices (U = 2, p = 0.0023, *delta* = 3.9153). There was one, albeit non-significant, outlier in the (*2R,6R*)-HNK-exposed group (Grubbs' $p > 0.05$) that accounted for the significant difference in group variances. Parametric assumptions were met upon its removal ($F_{(5,6)}$ = 2.245, p = 0.3532) and the mean difference between the VEH and (*2R,6R*)-HNK-exposed groups remained significantly different ($t_{(11)}$ = 4.215, p = 0.0014, g = 2.3462).

To assess whether changes in the probability of glutamate release contributed to the change in CA1 excitatory postsynaptic potentials upon (*2R,6R*)-HNK exposure, paired pulse stimuli were generated during baseline (t = 0 min) and following drug-superfusion (t = 30 min; Figure 4C). We found that the (*2R,6R*)-HNK-induced potentiation was associated with a significant and large-effect suppression of paired pulse facilitation relative to VEH-exposed slices (Figure 4B; $t_{(12)}$ = 6.214, $p < 0.0001$, d = 3.3216), which was significantly correlated with the extent of the potentiation observed (Figure 4D; R^2 = 0.3386, p = 0.0290).

At a synapse with a high probability of release, a single pulse will deplete the vesicles that are docked and primed for immediate release. With an interstimulus interval that is sufficiently brief (e.g., 50-ms, as used in the current study), the number of primed vesicles cannot be fully replenished upon the arrival of the second pulse; as a result, the second response is diminished/suppressed relative to the first (Creager et al., 1980; Kim and Alger, 2001). Thus, consistent with our prior observations using electrical field stimulation (Riggs et al., 2020), the decrease in paired pulse ratio in response to optogenetic stimulation suggests that (*2R,6R*)-HNK promotes the probability of glutamate release from CA1-projecting Schaffer collateral axon terminals.

4. DISCUSSION

(*2R,6R*)-HNK is a metabolite of ketamine that exerts behavioral, cellular, and synaptic effects that are implicated in its preclinical antidepressant-like actions (Highland et al., 2022). We hypothesize that (*2R,6R*)-HNK exerts its rapid antidepressant-like effects in part by promoting glutamate release at hippocampal Schaffer collateral synapses. Using electrical field stimulation, (*2R,6R*)-HNK promotes a persistent increase (~1.5 hr after drug wash-out) in glutamate release independent of NMDAR blockade or glutamatergic network

disinhibition (Riggs et al., 2020). In the current study, we used an optogenetic approach to establish that CA3 stimulation is sufficient for (*2R,6R*)-HNK to potentiate glutamate release in CA1. This study is the first to examine light-evoked activity-related changes in the subcircuit specific actions of (*2R,6R*)-HNK and provides additional support that Schaffer collateral synapses are an important site of antidepressant action.

In the hippocampus, (*2R,6R*)-HNK potentiates AMPAR-mediated activity (Riggs et al., 2020; Zanos et al., 2016) by promoting glutamate release at Schaffer collateral synapses independent of acute changes in AMPAR function (Riggs et al., 2020). Dual-pathway recordings revealed that this effect appears to be synapse-selective: The activity of CA1-projecting temporoammonic synapses (which arise from the entorhinal cortex and synapse onto distal dendrites of CA1 pyramidal neurons in the *stratum lacunosum moleculare*) is unchanged in response to acute (*2R,6R*)-HNK exposure, despite that Schaffer collateral synapses are faithfully potentiated by (*2R,6R*)-HNK at the same time within the same slice (Riggs et al., 2020). However, these studies used electrical field stimulation, so it is possible that concurrent activation of monoaminergic inputs could have contributed to the potentiation of glutamate release. This is because Schaffer collateral activity is modulated by extra-hippocampal afferents from dorsal raphe and locus coeruleus, the axons of which are retained in transverse hippocampal slice preparations *ex vivo* (Andersen et al., 2006). Given that (*2R,6R*)-HNK has been shown to promote the release of both serotonin and norepinephrine (Ago et al., 2019; Pham et al., 2018), it is possible that monoaminergic inputs could contribute to the changes in Shaffer collateral activity observed.

To address this, we targeted our stimulation selectively to CA3 neurons using ChrimsonR, a red-shifted channelrhodopsin that enables fast and reliable activation of discrete cell-types in acute brain slices (Klapoetke et al., 2014). We found that AAV-mediated expression of ChrimsonR-tdT under the Synapsin promoter allowed for select activation of CA3 neurons in the dorsal hippocampus. Direct application of (*2R,6R*)-HNK at an antidepressant-relevant concentration (10 μM; Lumsden et al., 2019) led to a rapid potentiation of CA1 excitatory postsynaptic potentials evoked by optical stimulation of ChrimsonR-expressing CA3 afferents. (*2R,6R*)-HNK suppressed optically-evoked paired-pulse facilitation at these CA3 projections, which further supports that the (*2R,6R*)-HNK-induced potentiation in CA1 is mediated in part by an increase in the probability of glutamate release from CA3 terminals. The current study demonstrates that (*2R,6R*)-HNK can promote glutamate release along CA1-projecting Schaffer collateral afferents in response to select optical excitation of CA3.

While the use of the Synapsin promoter sequence means we cannot completely rule out the contribution of interneurons (i.e., that may have also been labeled around the injection site), we observed strong preferential labeling of CA3 pyramidal neurons at the injection volume and titer used. We therefore conclude that the activity of this projection will not be markedly opposed by the coincident activation of labeled interneurons, if any. Additionally, light stimulation was targeted to axon terminals at the recording site in *stratum radiatum*, making coincident CA3 interneuron activation less likely. Our results indicate that (*2R,6R*)-HNK potentiates optically-evoked excitatory responses in area CA1 regardless of this possibility. Though not without its limitations (e.g., changes in normal cellular function, variability in

opsin expression, phototoxicity; Glasgow et al., 2019), optogenetic approaches can allow for more detailed investigation into the circuit-specific functions of putative antidepressants, such as (*2R,6R*)-HNK. These findings are the first to demonstrate proof-of-principle that genetically-encoded light-sensitive proteins can be used to establish the subcircuit specific plasticity induced by rapid-acting antidepressants.

(*2R,6R*)-HNK acts throughout the mesocorticolimbic system to alter the efficacy of synaptic transmission. This includes an acute increase in glutamate release in the hippocampus (Riggs et al., 2020), prefrontal cortex (Fukumoto et al., 2019; Pham et al., 2018), and ventrolateral periaqueductal gray (Chou et al., 2018; Ye et al., 2019) as well as a delayed enhancement in AMPAR expression in the hippocampus (Zanos et al., 2016) and ventrolateral periaqueductal gray (Chou et al., 2018; Ye et al., 2019). While (*2R,6R*)-HNK does not appear to directly modulate monoaminergic transporter activity (Can et al., 2016), it has been shown to promote the release of prefrontal serotonin and norepinephrine, but not dopamine (Ago et al., 2019; Pham et al., 2018). Consistent with this, while (*2R,6R*)-HNK suppresses glutamate release and AMPAR-mediated synaptic transmission in the ventral tegmental area, it does not alter firing of dopaminergic neurons in this region (Yao et al., 2018). These findings collectively suggest that (*2R,6R*)-HNK modulates monoaminergic synaptic transmission indirectly, likely via direct actions on glutamatergic signaling (Hess et al., 2021; López-Gil et al., 2019). Our findings support that (*2R,6R*)-HNK can act directly at Schaffer collateral presynaptic terminals to potentiate glutamate release, which we predict will then promote the activity of regions downstream of CA1.

More studies are needed to establish how the activity of mesocorticolimbic circuits contribute to the discrete behavioral effects of (*2R,6R*)-HNK. For instance, the hippocampus is most densely innervated by noradrenergic terminals originating from the locus coeruleus (Oleskevich et al., 1989) which modulate glutamatergic signaling (Drago et al., 2011) and enhance hippocampal synaptic plasticity (Hagena et al., 2016; Hansen, 2017). These projections have also been implicated in the pathophysiology of depression (Drago et al., 2011) and are a critical regulator of acute stress responsivity (Goddard et al., 2010). Ketamine enhances the hippocampal potentiation evoked by locus coeruleus activation (Frizzell and Harley, 1994) and directly potentiates the activity of locus coeruleus neurons (Iskandrani et al., 2015). These effects require AMPAR activation and are associated with an AMPAR-dependent enhancement in hippocampal release of norepinephrine and glutamate. Similar results have been reported in the prefrontal cortex (Kubota et al., 1999; Lorrain et al., 2003). In contrast, the local synaptic effects of (*2R,6R*)-HNK have so far been established either by direct infusion into a discrete brain region of interest (Chou et al., 2018; e.g., Fukumoto et al., 2019; Peng et al., 2022; Ye et al., 2019) or by direct bath application onto acute slices *ex vivo* (Chou, 2020; Chou et al., 2018; Peng et al., 2022; Riggs et al., 2020; Ye et al., 2019). Additional studies *ex vivo* and *in vivo* will be needed to provide a unified model for how (and across what time-scale; Wu et al., 2021) (*2R,6R*)-HNK modulates mesocorticolimbic circuit activity to elicit its antidepressant-like effects. These investigations will help clarify how rapid-acting antidepressant compounds promote functional reconfiguration and synaptic remodeling of regions that are causally implicated in the pathophysiology of depression (for a recent detailed review on this topic, see Parekh et al., 2022).

Overall, the literature (including the results of the present study) provides convergent evidence that (*2R,6R*)-HNK acts through a synergistic process that involves: (*a*) acute presynaptic mechanisms that promote neurotransmitter release, followed by (*b*) synaptogenic processes that then sustain the efficacy of synaptic transmission when (*2R,6R*)-HNK is no longer present (Hess et al., 2021; Highland et al., 2021). Essential to this process, is the rapid AMPAR activity-dependent release of neurotrophic factors, which has long been hypothesized as a potential mechanism to confer rapid antidepressant action (Alt et al., 2006) and has since proven necessary for the behavioral effects of (*2R,6R*)-HNK (Fukumoto et al., 2019; Zanos et al., 2016). The behavioral effects of (*2R,6R*)-HNK have been established in naïve mice in a number of behavioral tasks, including novelty-suppressed feeding (Aguilar-Valles et al., 2020; Fukumoto et al., 2019; Lumsden et al., 2019; Zanos et al., 2016), sucrose preference (Chou, 2020; Zanos et al., 2016, 2019a), female urine-sniffing (Chou, 2020; Fukumoto et al., 2019; Zanos et al., 2016), novelty exploration (Casarotto et al., 2021; Riggs et al., 2021), passive avoidance (Riggs et al., 2021), fear conditioning (Casarotto et al., 2021; Chen et al., 2020), and the forced swim test (Aguilar-Valles et al., 2020; Casarotto et al., 2021; Chen et al., 2020; Chou, 2020; Fukumoto et al., 2019; Herzog et al., 2021; Highland et al., 2022, 2018; Lumsden et al., 2019; Pham et al., 2018; Wulf et al., 2022; Zanos et al., 2019a, 2019b, 2016). Studies have also reported behavioral changes in animals that are categorized as stress-susceptible, including in the sucrose preference (Chou et al., 2018; Zanos et al., 2019a, 2019b, 2016; Zhong et al., 2021), female urine-sniffing (Peng et al., 2022; Zanos et al., 2016), learned helplessness (Chou et al., 2018; Elmer et al., 2020; Highland et al., 2018; Zanos et al., 2019a, 2019b, 2016), novelty exploration (Aleksandrova et al., 2020), social interaction (Zanos et al., 2016), and the forced swim- (Aleksandrova et al., 2020; Chou et al., 2018; Peng et al., 2022) and tail suspension tests (Peng et al., 2022). There are, however, studies that have not observed such behavioral effects of (*2R,6R*)-HNK (Shirayama and Hashimoto, 2018; Yamaguchi et al., 2018). It is pertinent that future studies begin to systematically account for potential experimental conditions or factors that could contribute to conflicting preclinical observations. It is likely that (*2R,6R*)-HNK exerts cell-type specific actions in discrete affective brain regions – but whose cooperative circuit interactions are needed to confer antidepressant-relevant behavioral adaptations via synaptogenic changes that broadly modify the function of those circuits (Parekh et al., 2022).

ACKNOWLEDGEMENTS

of any royalties that may be received by the University of Maryland, Baltimore. LMR and SMT declare no competing interests.

REFERENCES

Abdallah CG, Sanacora G, Duman RS, Krystal JH, 2018. The neurobiology of depression, ketamine and rapid-acting antidepressants: Is it glutamate inhibition or activation? Pharmacol Therapeut 190, 148–158. 10.1016/j.pharmthera.2018.05.010

Ago Y, Tanabe W, Higuchi M, Tsukada S, Tanaka T, Yamaguchi T, Igarashi H, Yokoyama R, Seiriki K, Kasai A, Nakazawa T, Nakagawa S, Hashimoto K, Hashimoto H, 2019. (R)-Ketamine Induces a Greater Increase in Prefrontal 5-HT Release Than (S)-Ketamine and Ketamine Metabolites via an AMPA Receptor-Independent Mechanism. Int J Neuropsychoph 22, 665–674. 10.1093/ijnp/pyz041

Aguilar-Valles A, Gregorio DD, Matta-Camacho E, Eslamizade MJ, Khlaifia A, Skaleka A, Lopez-Canul M, Torres-Berrio A, Bermudez S, Rurak GM, Simard S, Salmaso N, Gobbi G, Lacaille J-C, Sonenberg N, 2020. Antidepressant actions of ketamine engage cell-specific translation via eIF4E. Nature 1–5. 10.1038/s41586-020-03047-0

Aleksandrova LR, Wang YT, Phillips AG, 2020. Ketamine and its metabolite, (2R,6R)-HNK, restore hippocampal LTP and long-term spatial memory in the Wistar-Kyoto rat model of depression. Mol Brain 13, 92. 10.1186/s13041-020-00627-z [PubMed: 32546197]

Alt A, Nisenbaum ES, Bleakman D, Witkin JM, 2006. A role for AMPA receptors in mood disorders. Biochem Pharmacol 71, 1273–1288. 10.1016/j.bcp.2005.12.022 [PubMed: 16442080]

Andersen P, Morris R, Amaral D, Bliss T, O'Keefe J, 2006. The Hippocampus Book. 10.1093/acprof:oso/9780195100273.001.0001

Berman RM, Cappiello A, Anand A, Oren DA, Heninger GR, Charney DS, Krystal JH, 2000. Antidepressant effects of ketamine in depressed patients. Biol Psychiat 47, 351–354. 10.1016/s0006-3223(99)00230-9 [PubMed: 10686270]

Can A, Zanos P, Moaddel R, Kang HJ, Dossou KSS, Wainer IW, Cheer JF, Frost DO, Huang X-P, Gould TD, 2016. Effects of Ketamine and Ketamine Metabolites on Evoked Striatal Dopamine Release, Dopamine Receptors, and Monoamine Transporters. J Pharmacol Exp Ther 359, 159–170. 10.1124/jpet.116.235838 [PubMed: 27469513]

Casarotto PC, Girych M, Fred SM, Kovaleva V, Moliner R, Enkavi G, Biojone C, Cannarozzo C, Sahu MP, Kaurinkoski K, Brunello CA, Steinzeig A, Winkel F, Patil S, Vestring S, Serchov T, Diniz CRAF, Laukkanen L, Cardon I, Antila H, Rog T, Piepponen TP, Bramham CR, Normann C, Lauri SE, Saarma M, Vattulainen I, Castrén E, 2021. Antidepressant drugs act by directly binding to TRKB neurotrophin receptors. Cell. 10.1016/j.cell.2021.01.034

Chaki S, 2020. mGlu2/3 receptor as a novel target for rapid acting antidepressants. Adv Pharmacol 89, 289–309. 10.1016/bs.apha.2020.04.001 [PubMed: 32616210]

Chen BK, Luna VM, LaGamma CT, Xu X, Deng S-X, Suckow RF, Cooper TB, Shah A, Brachman RA, Mendez-David I, David DJ, Gardier AM, Landry DW, Denny CA, 2020. Sex-specific neurobiological actions of prophylactic (R,S)-ketamine, (2R,6R)-hydroxynorketamine, and (2S,6S)-hydroxynorketamine. Neuropsychopharmacol 1–13. 10.1038/s41386-020-0714-z

Chou D, 2020. Brain-derived neurotrophic factor in the ventrolateral periaqueductal gray contributes to (2R,6R)-hydroxynorketamine-mediated actions. Neuropharmacology 170, 108068. 10.1016/j.neuropharm.2020.108068 [PubMed: 32222405]

Chou D, Peng H-Y, Lin T-B, Lai C-Y, Hsieh M-C, Wen Y-C, Lee A-S, Wang H-H, Yang P-S, Chen G-D, Ho Y-C, 2018. (2R,6R)-hydroxynorketamine rescues chronic stress-induced depression-like behavior through its actions in the midbrain periaqueductal gray. Neuropharmacology 139, 1–12. 10.1016/j.neuropharm.2018.06.033 [PubMed: 29953886]

Cohen J, 1992. A power primer. Psychol Bull 112, 155–159. 10.1037//0033-2909.112.1.155 [PubMed: 19565683]

Cohen J, 1988. Statistical Power Analysis for the Behavioral Sciences. 10.4324/9780203771587

Creager R, Dunwiddie T, Lynch G, 1980. Paired-pulse and frequency facilitation in the CA1 region of the in vitro rat hippocampus. J Physiology 299, 409–424. 10.1113/jphysiol.1980.sp013133

Cristea IA, Naudet F, 2019. US Food and Drug Administration approval of esketamine and brexanolone. Lancet Psychiatry 6, 975–977. 10.1016/s2215-0366(19)30292-5 [PubMed: 31680013]

Drago A, Crisafulli C, Sidoti A, Serretti A, 2011. The molecular interaction between the glutamatergic, noradrenergic, dopaminergic and serotoninergic systems informs a detailed genetic perspective on depressive phenotypes. Prog Neurobiol 94, 418–460. 10.1016/j.pneurobio.2011.05.009 [PubMed: 21723912]

Duman RS, Shinohara R, Fogaça MV, Hare B, 2019. Neurobiology of rapid-acting antidepressants: convergent effects on GluA1-synaptic function. Mol Psychiatr 24, 1816–1832. 10.1038/s41380-019-0400-x

Elmer GI, Tapocik JD, Mayo CL, Zanos P, Gould TD, 2020. Ketamine metabolite (2R,6R)-hydroxynorketamine reverses behavioral despair produced by adolescent trauma. Pharmacol Biochem Be 196, 172973. 10.1016/j.pbb.2020.172973

Frizzell LM, Harley CW, 1994. The N-methyl-d-aspartate channel blocker ketamine does not attenuate, but enhances, locus coeruleus-induced potentiation in rat dentate gyrus. Brain Res 663, 173–178. 10.1016/0006-8993(94)90476-6 [PubMed: 7531596]

Fukumoto K, Fogaça MV, Liu R-J, Duman C, Kato T, Li X-Y, Duman RS, 2019. Activity-dependent brain-derived neurotrophic factor signaling is required for the antidepressant actions of (2R,6R)-hydroxynorketamine. Proc National Acad Sci 116, 297–302. 10.1073/pnas.1814709116

Glasgow SD, McPhedrain R, Madranges JF, Kennedy TE, Ruthazer ES, 2019. Approaches and Limitations in the Investigation of Synaptic Transmission and Plasticity. Frontiers Synaptic Neurosci 11, 20. 10.3389/fnsyn.2019.00020

Goddard AW, Ball SG, Martinez J, Robinson MJ, Yang CR, Russell JM, Shekhar A, 2010. Current perspectives of the roles of the central norepinephrine system in anxiety and depression. Depress Anxiety 27, 339–350. 10.1002/da.20642 [PubMed: 19960531]

Gould TD, Zarate JCA, Thompson SM, 2019. Molecular Pharmacology and Neurobiology of Rapid-Acting Antidepressants. Annu Rev Pharmacol 59, 213–236. 10.1146/annurev-pharmtox-010617-052811

Hagena H, Hansen N, Manahan-Vaughan D, 2016. β-Adrenergic Control of Hippocampal Function: Subserving the Choreography of Synaptic Information Storage and Memory. Cereb Cortex New York Ny 26, 1349–1364. 10.1093/cercor/bhv330

Hansen N, 2017. The Longevity of Hippocampus-Dependent Memory Is Orchestrated by the Locus Coeruleus-Noradrenergic System. Neural Plast 2017, 2727602. 10.1155/2017/2727602 [PubMed: 28695015]

Hashimoto K, 2019. Rapid-acting antidepressant ketamine, its metabolites and other candidates: A historical overview and future perspective. Psychiat Clin Neuros 73, 613–627. 10.1111/pcn.12902

Henter ID, Park LT, Zarate CA, 2021. Novel Glutamatergic Modulators for the Treatment of Mood Disorders: Current Status. Cns Drugs 1–17. 10.1007/s40263-021-00816-x

Herzog DP, Perumal N, Manicam C, Treccani G, Nadig J, Rossmanith M, Engelmann J, Jene T, Hasch A, van der Kooij MA Lieb K, Gassen NC, Grus FH, Müller MB, 2021. Longitudinal CSF proteome profiling in mice to uncover the acute and sustained mechanisms of action of rapid acting antidepressant (2R,6R)-hydroxynorketamine (HNK). Neurobiology Stress 15, 100404. 10.1016/j.ynstr.2021.100404

Hess EM, Riggs LM, Michaelides M, Gould TD, 2021. Mechanisms of Ketamine and its Metabolites as Antidepressants. Biochem Pharmacol 114892. 10.1016/j.bcp.2021.114892 [PubMed: 34968492]

Highland JN, Morris PJ, Konrath KM, Riggs LM, Hagen NR, Zanos P, Powels CF, Moaddel R, Thomas CJ, Wang AQ, Gould TD, 2022. Hydroxynorketamine Pharmacokinetics and Antidepressant Behavioral Effects of (2,6)- and (5R)-Methyl-(2R,6R)-hydroxynorketamines. Acs Chem Neurosci. 10.1021/acschemneuro.1c00761

Highland JN, Morris PJ, Zanos P, Lovett J, Ghosh S, Wang AQ, Zarate JCA, Thomas CJ, Moaddel R, Gould TD, 2018. Mouse, rat, and dog bioavailability and mouse oral antidepressant efficacy of (2R,6R)-hydroxynorketamine. J Psychopharmacol 33, 269881118812095–269881118812095. 10.1177/0269881118812095

Highland JN, Zanos P, Riggs LM, Georgiou P, Clark SM, Morris PJ, Moaddel R, Thomas CJ, Zarate CA, Pereira EFR, Gould TD, 2021. Hydroxynorketamines: Pharmacology and Potential Therapeutic Applications. Pharmacol Rev 73, 763–791. 10.1124/pharmrev.120.000149 [PubMed: 33674359]

Iskandrani KSE, Oosterhof CA, Mansari ME, Blier P, 2015. Impact of subanesthetic doses of ketamine on AMPA-mediated responses in rats: An in vivo electrophysiological study on monoaminergic and glutamatergic neurons. J Psychopharmacol 29, 792–801. 10.1177/0269881115573809 [PubMed: 25759403]

Kim J, Alger BE, 2001. Random Response Fluctuations Lead to Spurious Paired-Pulse Facilitation. J Neurosci 21, 9608–9618. 10.1523/jneurosci.21-24-09608.2001 [PubMed: 11739571]

Klapoetke NC, Murata Y, Kim SS, Pulver SR, Birdsey-Benson A, Cho YK, Morimoto TK, Chuong AS, Carpenter EJ, Tian Z, Wang J, Xie Y, Yan Z, Zhang Y, Chow BY, Surek B, Melkonian M, Jayaraman V, Constantine-Paton M, Wong GK-S, Boyden ES, 2014. Independent Optical Excitation of Distinct Neural Populations. Nat Methods 11, 338–346. 10.1038/nmeth.2836 [PubMed: 24509633]

Krystal JH, Karper LP, Seibyl JP, Freeman GK, Delaney R, Bremner JD, Heninger GR, Bowers MB, Charney DS, 1994. Subanesthetic Effects of the Noncompetitive NMDA Antagonist, Ketamine, in Humans. Arch Gen Psychiat 51, 199. 10.1001/archpsyc.1994.03950030035004 [PubMed: 8122957]

Kubota T, Anzawa N, Hirota K, Yoshida H, Kushikata T, Matsuki A, 1999. Effects of ketamine and pentobarbital on noradrenaline release from the medial prefrontal cortex in rats. Can J Anaesth 46, 388–392. 10.1007/bf03013235 [PubMed: 10232727]

Lener MS, Kadriu B, Zarate JCA, 2017. Ketamine and Beyond: Investigations into the Potential of Glutamatergic Agents to Treat Depression. Drugs 77, 381–401. 10.1007/s40265-017-0702-8 [PubMed: 28194724]

López-Gil X, Jiménez-Sánchez L, Campa L, Castro E, Frago C, Adell A, 2019. Role of Serotonin and Noradrenaline in the Rapid Antidepressant Action of Ketamine. Acs Chem Neurosci 10, 3318–3326. 10.1021/acschemneuro.9b00288 [PubMed: 31244055]

Lorrain DS, Baccei CS, Bristow LJ, Anderson JJ, Varney MA, 2003. Effects of ketamine and n-methyl-d-aspartate on glutamate and dopamine release in the rat prefrontal cortex: modulation by a group II selective metabotropic glutamate receptor agonist LY379268. Neuroscience 117, 697–706. 10.1016/s0306-4522(02)00652-8 [PubMed: 12617973]

Lumsden EW, Troppoli TA, Myers SJ, Zanos P, Aracava Y, Kehr J, Lovett J, Kim S, Wang F-H, Schmidt S, Jenne CE, Yuan P, Morris PJ, Thomas CJ, Zarate JCA, Moaddel R, Traynelis SF, Pereira EFR, Thompson SM, Albuquerque EX, Gould TD, 2019. Antidepressant-relevant concentrations of the ketamine metabolite (2R,6R)-hydroxynorketamine do not block NMDA receptor function. Proc National Acad Sci 116, 5160–5169. 10.1073/pnas.1816071116

McIntyre RS, Rosenblat JD, Nemeroff CB, Sanacora G, Murrough JW, Berk M, Brietzke E, Dodd S, Gorwood P, Ho R, Iosifescu DV, Jaramillo CL, Kasper S, Kratiuk K, Lee JG, Lee Y, Lui LMW, Mansur RB, Papakostas GI, Subramaniapillai M, Thase M, Vieta E, Young AH, Zarate CA, Stahl S, 2021. Synthesizing the Evidence for Ketamine and Esketamine in Treatment-Resistant Depression: An International Expert Opinion on the Available Evidence and Implementation. Am J Psychiat 178, 383–399. 10.1176/appi.ajp.2020.20081251 [PubMed: 33726522]

Morris PJ, Moaddel R, Zanos P, Moore CE, Gould TD, Zarate JCA, Thomas CJ, 2017. Synthesis and N-Methyl-d-aspartate (NMDA) Receptor Activity of Ketamine Metabolites. Org Lett 19, 4572–4575. 10.1021/acs.orglett.7b02177 [PubMed: 28829612]

Murrough JW, Abdallah CG, Mathew SJ, 2017. Targeting glutamate signalling in depression: progress and prospects. Nat Rev Drug Discov 16, 472–486. 10.1038/nrd.2017.16 [PubMed: 28303025]

Newport DJ, Carpenter LL, McDonald WM, Potash JB, Tohen M, Nemeroff CB, Treatments, T.A.C. of R.T.F. on N.B. and, 2015. Ketamine and Other NMDA Antagonists: Early Clinical Trials and Possible Mechanisms in Depression. Am J Psychiat 172, 950–966. 10.1176/appi.ajp.2015.15040465 [PubMed: 26423481]

Oleskevich S, Descarries L, Lacaille J, 1989. Quantified distribution of the noradrenaline innervation in the hippocampus of adult rat. J Neurosci 9, 3803–3815. 10.1523/jneurosci.09-11-03803.1989 [PubMed: 2585056]

Parekh PK, Johnson SB, Liston C, 2022. Synaptic Mechanisms Regulating Mood State Transitions in Depression. Annu Rev Neurosci 45. 10.1146/annurev-neuro-110920-040422

Peng W-H, Kan H-W, Ho Y-C, 2022. Periaqueductal gray is required for controlling chronic stress-induced depression-like behavior. Biochem Bioph Res Co. 10.1016/j.bbrc.2022.01.025

Pham TH, Defaix C, Xu X, Deng S-X, Fabresse N, Alvarez J-C, Landry DW, Brachman RA, Denny CA, Gardier AM, 2018. Common Neurotransmission Recruited in (R,S)-Ketamine and (2R,6R)-Hydroxynorketamine-Induced Sustained Antidepressant-like Effects. Biol Psychiat 84, e3–e6. 10.1016/j.biopsych.2017.10.020 [PubMed: 29174592]

Riggs LM, An X, Pereira EFR, Gould TD, 2021. (R,S)-ketamine and (2R,6R)-hydroxynorketamine differentially affect memory as a function of dosing frequency. Transl Psychiat 11, 583. 10.1038/s41398-021-01685-0

Riggs LM, Aracava Y, Zanos P, Fischell J, Albuquerque EX, Pereira EFR, Thompson SM, Gould TD, 2020. (2R,6R)-hydroxynorketamine rapidly potentiates hippocampal glutamatergic transmission through a synapse-specific presynaptic mechanism. Neuropsychopharmacol 10.1038/s41386-019-0443-3. 10.1038/s41386-019-0443-3

Riggs LM, Gould TD, 2021. Ketamine and the Future of Rapid-Acting Antidepressants. Annu Rev Clin Psycho 17, 1–25. 10.1146/annurev-clinpsy-072120-014126

Shirayama Y, Hashimoto K, 2018. Lack of Antidepressant Effects of (2R,6R)-Hydroxynorketamine in a Rat Learned Helplessness Model: Comparison with (R)-Ketamine. Int J Neuropsychoph 21, 84–88. 10.1093/ijnp/pyx108

Skolnick P, Popik P, Trullas R, 2009. Glutamate-based antidepressants: 20 years on. Trends Pharmacol Sci 30, 563–569. 10.1016/j.tips.2009.09.002 [PubMed: 19837463]

Witkin JM, Martin AE, Golani LK, Xu NZ, Smith JL, 2019. Chapter Three Rapid-acting antidepressants. Adv Pharmacol 86, 47–96. 10.1016/bs.apha.2019.03.002 [PubMed: 31378256]

Wu H, Savalia NK, Kwan AC, 2021. Ketamine for a Boost of Neural Plasticity: How, but Also When? Biol Psychiat 89, 1030–1032. 10.1016/j.biopsych.2021.03.014 [PubMed: 34016377]

Wulf HA, Browne CA, Zarate CA, Lucki I, 2022. Mediation of the behavioral effects of ketamine and (2R,6R)-hydroxynorketamine in mice by kappa opioid receptors. Psychopharmacology 1–8. 10.1007/s00213-022-06118-4

Yamaguchi J-I, Toki H, Qu Y, Yang C, Koike H, Hashimoto K, Mizuno-Yasuhira A, Chaki S, 2018. (2R,6R)-Hydroxynorketamine is not essential for the antidepressant actions of (R)-ketamine in mice. Neuropsychopharmacol 43, 1900–1907. 10.1038/s41386-018-0084-y

Yao N, Skiteva O, Zhang X, Svenningsson P, Chergui K, 2018. Ketamine and its metabolite (2R,6R)-hydroxynorketamine induce lasting alterations in glutamatergic synaptic plasticity in the mesolimbic circuit. Mol Psychiatr 23, 2066–2077. 10.1038/mp.2017.239

Ye L, Ko C-Y, Huang Y, Zheng C, Zheng Y, Chou D, 2019. Ketamine metabolite (2R,6R)-hydroxynorketamine enhances aggression via periaqueductal gray glutamatergic transmission. Neuropharmacology 157, 107667–107667. 10.1016/j.neuropharm.2019.107667 [PubMed: 31207251]

Zanos P, Highland JN, Liu X, Troppoli TA, Georgiou P, Lovett J, Morris PJ, Stewart BW, Thomas CJ, Thompson SM, Moaddel R, Gould TD, 2019a. (R)-Ketamine exerts antidepressant actions partly via conversion to (2R,6R)-hydroxynorketamine, while causing adverse effects at sub-anaesthetic doses. Brit J Pharmacol 176, 2573–2592. 10.1111/bph.14683 [PubMed: 30941749]

Zanos P, Highland JN, Stewart BW, Georgiou P, Jenne CE, Lovett J, Morris PJ, Thomas CJ, Moaddel R, Zarate JCA, Gould TD, 2019b. (2R,6R)-hydroxynorketamine exerts mGlu(2) receptor-dependent antidepressant actions. Proc National Acad Sci 116, 6441–6450. 10.1073/pnas.1819540116

Zanos P, Moaddel R, Morris PJ, Georgiou P, Fischell J, Elmer GI, Alkondon M, Yuan P, Pribut HJ, Singh NS, Dossou KSS, Fang Y, Huang X-P, Mayo CL, Wainer IW, Albuquerque EX, Thompson SM, Thomas CJ, Zarate JCA, Gould TD, 2016. NMDAR inhibition-independent antidepressant actions of ketamine metabolites. Nature 533, 481–486. 10.1038/nature17998 [PubMed: 27144355]

Zanos P, Moaddel R, Morris PJ, Riggs LM, Highland JN, Georgiou P, Pereira EFR, Albuquerque EX, Thomas CJ, Zarate JCA, Gould TD, 2018. Ketamine and Ketamine Metabolite Pharmacology:

Insights into Therapeutic Mechanisms. Pharmacol Rev 70, 621–660. 10.1124/pr.117.015198 [PubMed: 29945898]

Zarate CA, 2021. Glutamate modulators and beyond: A neuroscience revolution in the making. Eur Neuropsychopharm. 10.1016/j.euroneuro.2021.09.005

Zarate CA, Singh JB, Carlson PJ, Brutsche NE, Ameli R, Luckenbaugh DA, Charney DS, Manji HK, 2006. A randomized trial of an N-methyl-D-aspartate antagonist in treatment-resistant major depression. Arch Gen Psychiat 63, 856–64. 10.1001/archpsyc.63.8.856 [PubMed: 16894061]

Zhong X, Ouyang C, Liang W, Dai C, Zhang W, 2021. (2R,6R)-Hydroxynorketamine Alleviates Electroconvulsive Shock-Induced Learning Impairment by Inhibiting Autophagy. Neuropsych Dis Treat Volume 17, 297–304. 10.2147/ndt.s278422

Stereotaxic Surgery

Acute Slice Electrophysiology

28 Days

Infusion of AAV into CA3 of Dorsal Hippocampus

Syn-ChrimsonR-tdT

CA1

CA3

Extract Hippocampi

Record Optically-Evoked Excitatory Responses

CA1

CA3

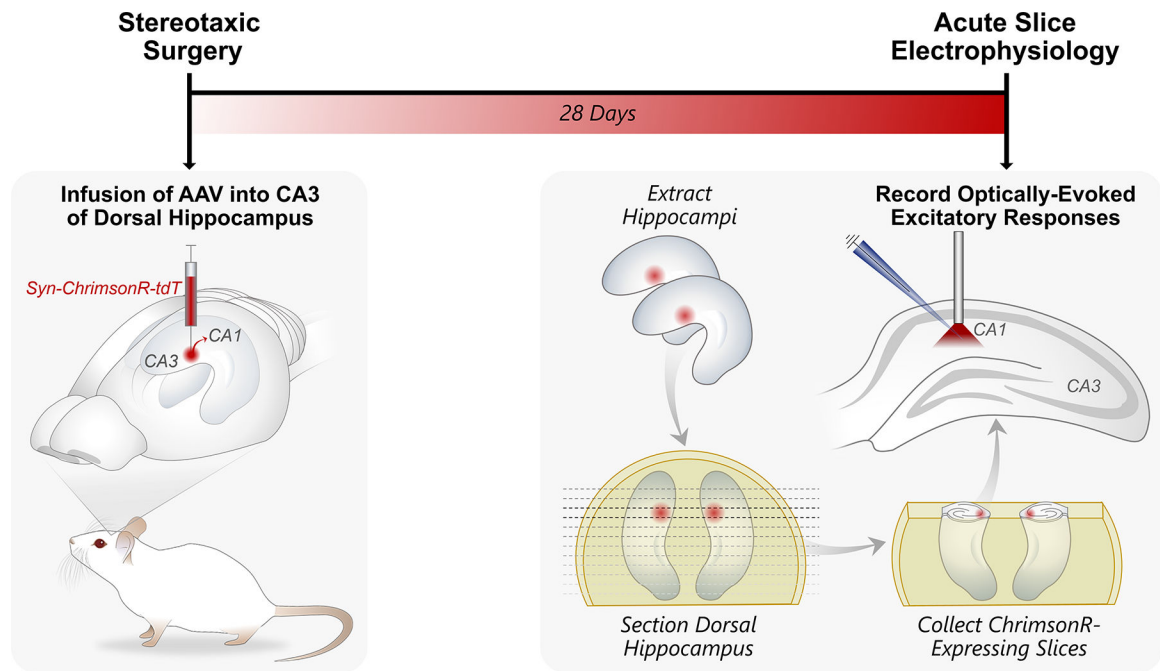*Section Dorsal Hippocampus*

Collect ChrimsonR-Expressing Slices

Figure 1. Experimental Timeline.

pAAV-Syn-ChrimsonR-tdT was infused into the CA3 region of the dorsal hippocampus of five-week-old male Sprague Dawley rats. Four weeks later, transverse dorsal hippocampal slices were collected for *ex vivo* electrophysiology recordings. ChrimsonR-expressing CA3 afferents were optically stimulated using a fiber-coupled 625 nm LED and excitatory postsynaptic potentials were recorded in CA1 *stratum radiatum*.
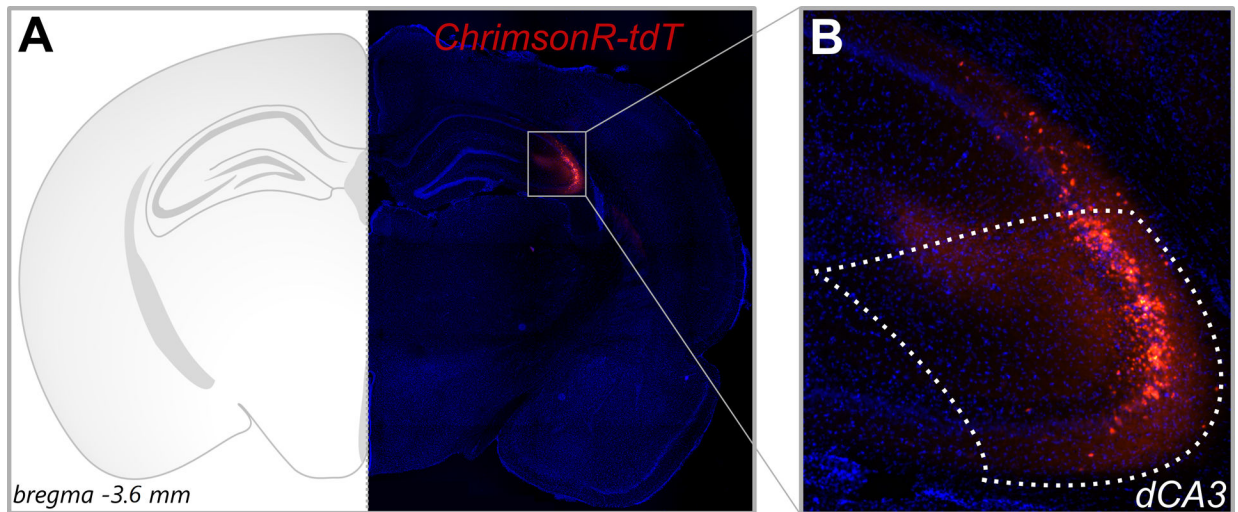
Figure 2. ChrimsonR-tdT expression in CA3 neurons of the dorsal hippocampus.
pAAV-Syn-ChrimsonR-tdT was infused into the CA3 region of the dorsal hippocampus of five-week-old adult male Sprague Dawley rats. **(A)** Representative image of ChrimsonR-tdT expression (*bregma –3.8 mm*) at 4× magnification against DAPI staining. **(B)** Section demarcated in Panel A at 10× magnification. A slow (0.025 μl/min) low-volume (0.3 μl) infusion led to spatial restriction of ChrimsonR-tdT in dorsal CA3 (dCA3) neurons.
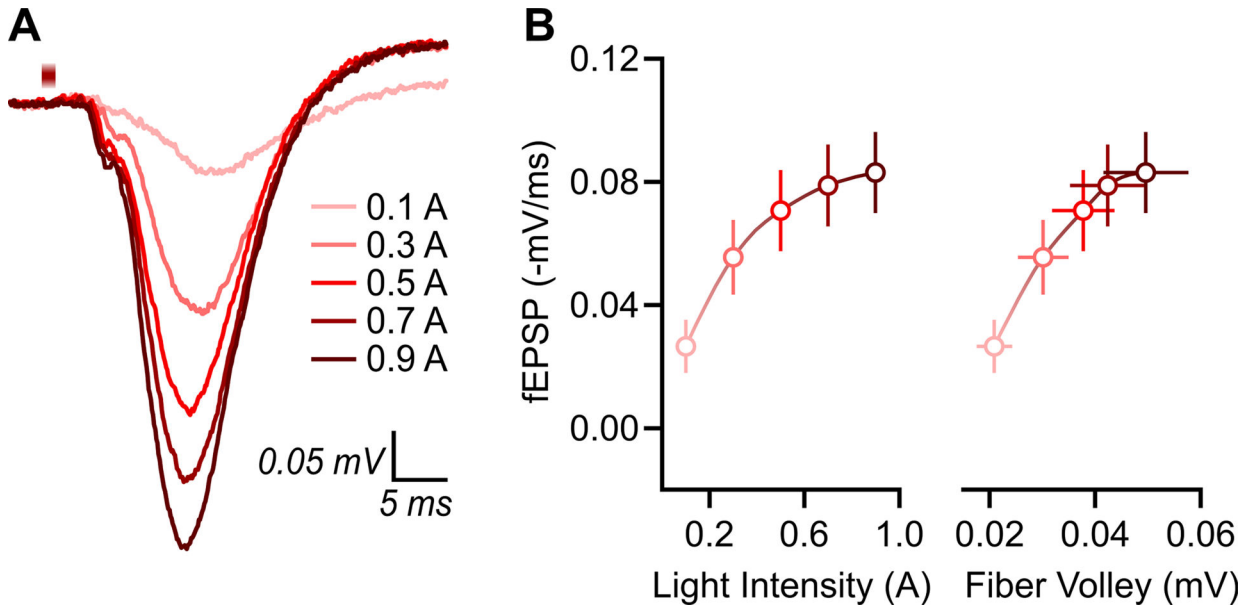
Figure 3. CA1 excitatory postsynaptic potentials in response to select optical stimulation of CA3 neurons.

CA1 excitatory postsynaptic potentials were evoked *ex vivo* using 625 nm LED light stimulation of ChrimsonR-expressing CA3 neurons (1 ms duration, 0.05 Hz interval, 5 mW/mm^2 irradiance). **(A)** Representative response traces at increasing light stimulation intensity. **(B)** Input-output relationship (*n* = 14) using 0.2-A current steps (*left panel*) and plotted against fiber volley amplitude in mV (*right panel*). Data are presented as mean ± standard error of the mean and the data points are fit with a smoothing spline curve. Note, field potentials are generated by negative-going/inward current, but are presented here as positive values for ease of interpretation; (−) is included as a prefix to mV/ms to indicate that the raw values are negative.
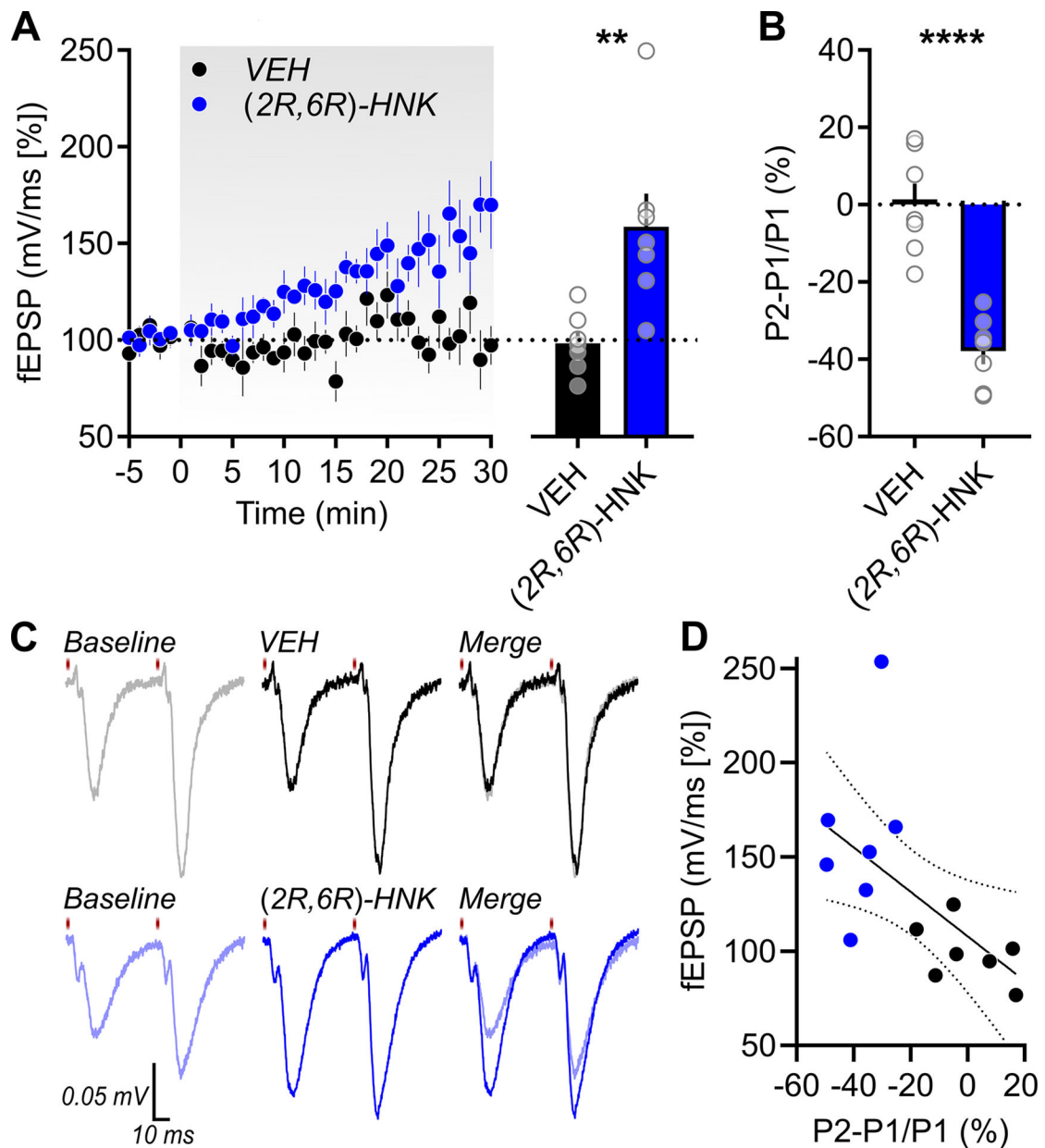
Figure 4. (2R,6R)-hydroxynorketamine rapidly potentiates optically-evoked Schaffer collateral synaptic activity.

A combined optogenetic and electrophysiological approach was used to assess the effects of (*2R,6R*)-hydroxynorketamine (HNK) on optically-evoked responses in CA1 *stratum radiatum*. **(A)** Relative to vehicle (VEH)-exposed slices ($n = 7$ slices from 4 rats), a 30-min superfusion of (*2R,6R*)-hydroxynorketamine (HNK; $n = 7$ slices from 4 rats) led to a significant potentiation of optically-evoked CA1 excitatory postsynaptic potentials. **(B,C)** (*2R,6R*)-HNK suppressed paired pulse facilitation (50-ms interstimulus interval) which **(D)** correlated with the extent of the potentiation observed ($R^2 = 0.3386$, linear regression ± 95% CI). Data are presented as mean + standard error of the mean and significance is defined as **$p = 0.0023$ and ****$p < 0.0001$.